SIAM J. NUMER. ANAL.
Vol. 58, No. 1, pp. 788–810

A PROOF THAT ANDERSON ACCELERATION IMPROVES THE CONVERGENCE RATE IN LINEARLY CONVERGING FIXED-POINT METHODS (BUT NOT IN THOSE CONVERGING QUADRATICALLY)*

CLAIRE EVANS†, SARA POLLOCK‡, LEO G. REBHOLZ†, AND MENGYING XIAO‡

Abstract. This paper provides theoretical justification that Anderson acceleration (AA) improves the convergence rate of contractive fixed-point iterations in the vicinity of a fixed-point. AA has been used for decades to speed up nonlinear solvers in many applications. However, a rigorous mathematical justification of the improved convergence rate has remained lacking. The key ideas of the analysis presented here are relating the difference of consecutive iterates to residuals based on performing the inner-optimization in a Hilbert space setting, and explicitly defining the gain in the optimization stage to be the ratio of improvement over a step of the unaccelerated fixed-point iteration. The main result shown here is that AA improves the convergence rate of a fixed-point iteration to first order by a factor of the gain at each step. While the acceleration reduces the contribution from the first-order terms in the residual expansion, additional superlinear terms arise. In agreement with the theory, numerical tests are given which illustrate improved linear convergence rates, but for quadratically converging fixed-point iterations the rate is slowed. Our tests further illustrate how AA can perform similarly to damping in enlarging the domain of convergence.

Key words. Anderson acceleration, fixed-point iterations, nonlinear iterations, convergence theory, damping

AMS subject classification. 65J15

DOI. 10.1137/19M1245384

1. Introduction.

We study an acceleration technique for fixed-point problems called Anderson acceleration, in which a history of search-directions is used to improve the rate of convergence of fixed-point iterations. The method was originally introduced by Anderson in 1965 in the context of integral equations [3]. It has recently been used in many applications, including multisecant methods for fixed-point iterations in electronic structure computations [8], geometry optimization problems [16], various types of flow problems [15, 17], radiation diffusion and nuclear physics [2, 19], molecular interaction [18], machine learning [9], improving the alternating projections method for computing nearest correlation matrices [11], and on a wide range of nonlinear problems in the context of generalized minimal residual (GMRES) methods in [21]. We further refer readers to [12, 14, 15, 21] and references therein for detailed discussions on both practical implementation and a history of the method and its applications.

After a long history of use and a strong recent interest, the first mathematical convergence results for Anderson acceleration (for both linear and nonlinear problems) appear in 2015 in [20], under the usual local assumptions for convergence of Newton

*Received by the editors February 19, 2019; accepted for publication (in revised form) November 19, 2019; published electronically February 20, 2020.
https://doi.org/10.1137/19M1245384
Funding: The work of the second author was partially supported by the National Science Foundation grant DMS-1852876. The work of the third author was partially supported by the National Science Foundation grant DMS-1522191.

†School of Mathematical and Statistical Sciences, Clemson University, Clemson, SC 29634 (cevans4@g.clemson.edu, rebholz@clemson.edu).
‡Department of Mathematics, University of Florida, Gainesville, FL 32611 (s.pollock@ufl.edu, m.xiao@ufl.edu).

iterations. However, this theory does not prove that Anderson acceleration improves the convergence of a fixed-point iteration, or in other words accelerates convergence in the sense of [6]. Rather, it proves that Anderson accelerated fixed-point iterations will converge in the neighborhood of a fixed-point; and an upper bound on the convergence rate is shown to approach from above the convergence rate of the underlying fixed-point iteration. While an important stage in the developing theory, this does not explain the efficacy of the method, which has gained popularity as practitioners have continued to observe an often dramatic speedup and increase in robustness from Anderson acceleration over a wide range of problems.

The purpose of this paper is to address this gap in the theory by proving an estimate for Anderson acceleration that shows, in the vicinity of the solution, an improvement in the convergence rate for fixed-point iterations (for general C^1 functions with Lipschitz derivatives) that converge linearly (with rate κ); or to a damped iteration where κ is replaced by $((1-\beta_{k-1})+\beta_{k-1}\kappa)$, for damping (mixing) parameter $0<\beta_{k-1}\leq 1$. By explicitly defining the gain of the optimization stage at iteration k to be the ratio θ_k of the optimized objective function compared to that of the usual fixed-point method, the residual norm at step k is shown to be reduced approximately by $\theta_k((1-\beta_{k-1})+\beta_{k-1}\kappa)$, near the solution, where $\beta_{k-1}=1$ produces the undamped iteration. The key ideas to the proof are an expansion of the residual errors, developing expressions relating the difference of consecutive iterates and residuals, and explicitly factoring in the gain from the optimization stage. A somewhat similar approach is used by the authors to prove that Anderson acceleration improves Picard iteration convergence for finite element discretizations of the steady Navier–Stokes equations in [17] (without the Lipschitz assumption on the derivative of the fixed-point operator), and herein these ideas are extended to more general fixed-point iterations.

Consistent with the presented analysis which indicates that Anderson acceleration introduces higher-order error terms, our numerical results illustrate Anderson acceleration slowing the convergence of quadratically convergent Newton iterations. In the first part of the theory presented below we consider the damped Anderson iteration (in the literature the damping parameter for Anderson is often called the mixing parameter). This is motivated by the observation that for noncontractive fixed-point iterations, the Anderson accelerated iteration is more robust with respect to choice of damping (mixing) parameter than the unaccelerated iteration [10, 19], but may still require some degree of damping for convergence.

This paper is arranged as follows. In section 2, we review Anderson acceleration, describe the problem setting, and give some basic definitions and notation. Section 3 gives several important technical results to make the later analysis cleaner and simpler. Section 4 gives the main result of the paper, showing how the linear convergence rate is improved by Anderson acceleration, although additional higher-order error terms arise. Section 5 gives results from numerical tests, with the intent of illustrating the current contributions to the theory. Conclusions are given in the final section.

2. Anderson acceleration. In what follows, we will consider a fixed-point operator $g : X \to X$, where X is a Hilbert space with norm $\|\cdot\|$ and inner-product $(\cdot,\cdot)$. The Anderson acceleration algorithm with depth m applied to the fixed-point problem $g(x)=x$ reads as follows.

ALGORITHM 2.1 (Anderson iteration). *The Anderson acceleration with depth $m\geq 0$ and damping factors $0<\beta_k\leq 1$ reads as follows:*

Step 0: Choose $x_0\in X$.

Step 1: Find $\tilde{x}_1\in X$ such that $\tilde{x}_1=g(x_0)$. Set $x_1=\tilde{x}_1$.

Step $k+1$: For $k = 1, 2, 3, \ldots$ set $m_k = \min\{k, m\}$.
(a) *Find $\tilde{x}_{k+1} = g(x_k)$.*
(b) *Solve the minimization problem for $\{\alpha_j^{k+1}\}_{k-m_k}^{k}$,*

$$\min_{\sum_{j=k-m_k}^{k} \alpha_j^{k+1}=1} \left\| \sum_{j=k-m_k}^{k} \alpha_j^{k+1}(\tilde{x}_{j+1} - x_j) \right\|. \tag{2.1}$$

(c) *For damping factor $0 < \beta_k \leq 1$, set*

$$x_{k+1} = (1-\beta_k) \sum_{j=k-m_k}^{k} \alpha_j^{k+1} x_j + \beta_k \sum_{j=k-m_k}^{k} \alpha_j^{k+1} \tilde{x}_{j+1}. \tag{2.2}$$

Throughout this work, we will use the stage-k residual and error terms

$$e_k \coloneqq x_k - x_{k-1}, \quad \tilde{e}_k \coloneqq \tilde{x}_k - \tilde{x}_{k-1}, \quad w_k \coloneqq \tilde{x}_k - x_{k-1}. \tag{2.3}$$

Define the following averages given by the solution $\alpha^{k+1} = \{\alpha_j^{k+1}\}_{j=k-m_k}^{k}$ to the optimization problem (2.1) by

(2.4)
$$x_k^{\alpha} = \sum_{j=k-m_k}^{k} \alpha_j^{k+1} x_j, \quad \tilde{x}_{k+1}^{\alpha} = \sum_{j=k-m_k}^{k} \alpha_j^{k+1} \tilde{x}_{j+1}, \quad w_{k+1}^{\alpha} = \sum_{j=k-m_k}^{k} \alpha_j^{k+1}(g(x_j) - x_j).$$

Then the update (2.2) can be written in terms of the averages x^{α} and $\tilde{x}^{\alpha}$,

$$x_{k+1} = (1-\beta_k) x_k^{\alpha} + \beta_k \tilde{x}_{k+1}^{\alpha}, \tag{2.5}$$

and the stage-k gain θ_k can be defined by

$$\|w_k^{\alpha}\| = \theta_k \|w_k\|. \tag{2.6}$$

The key to showing the acceleration of this technique defined by taking a linear combination of a history of steps corresponding to the coefficients of the optimization problem (2.1) is connecting the gain θ_k given by (2.6) to the differences of consecutive iterates and residual terms in (2.4). As such, the success (or failure) of the algorithm to reduce the residual is coupled to the success of the optimization problem at each stage of the algorithm. As $\alpha_k^{k+1} = 1, \alpha_j^{k+1} = 0, j \neq k$, is in the feasible set for (2.1), it follows immediately that $0 \leq \theta_k \leq 1$. As discussed in the remainder, the improvement in the contraction rate of the fixed-point iteration is characterized by θ_k.

The two main components of the proof of residual convergence at an accelerated rate are the expansion of the residual w_{k+1} into w_k^{α} and error terms $e_{k-m_{k-1}}, \ldots, e_k$; and control of the e_j's in terms of the corresponding w_j's. In the next section, the first of these is established for general m, and the second for the particular cases of depth $m = 1$ and $m = 2$, with the result then shown for general m.

3. Technical preliminaries. There are two main technical results used in our theory. The first is an expansion of the residual, and the second is a set of estimates relating the difference of consecutive iterates to residuals. These are shown in sections 3.1 and 3.2, respectively. The main results which depend on these estimates are then presented in section 4.

For the bounds in section 3.2 relating the difference of consecutive iterates to residuals, the operator $g : X \to X$ is assumed to be Lipschitz continuous and contractive, as in [17]; see Assumption 3.2 below. The results of section 3.1 do not require the contractive property, but require the assumption that g is continuously differentiable with a uniformly Lipschitz derivative to allow for Taylor expansions leading to bounds on the error terms. We denote the derivative of g by $g'(\cdot;\cdot)$, and employ the standard notation that form $g'(\cdot;\cdot)$ is linear with respect to the argument to the right of the semicolon.

Assumption 3.1. Let X be a Hilbert space and let $g : X \to X$. Assume g has a fixed-point $x^* \in X$, and there are positive constants κ and $\hat{\kappa}$ with

1. $g \in C^1(X)$,
2. $\|g'(y;u)\| \le \kappa \|u\|$ for each y and all $u \in X$,
3. $\|g'(x;u) - g'(y,u)\| \le \hat{\kappa} \|x-y\| \|u\|$ for each x, y and all $u \in X$.

Assumption 3.2. Let X be a Hilbert space and let $g : X \to X$. Assume $\|g(y) - g(x)\| \le \kappa \|x - y\|$ for every $x, y \in X$, with $\kappa < 1$.

By standard fixed-point theory, Assumption 3.2 implies the existence of a unique fixed-point x^* of g in X. In a slight abuse of notation, the difference of consecutive iterates, $e_k = x_k - x_{k-1}$, is loosely referred to in this manuscript as an error term. As shown carefully in [17], the true error $x_k - x^*$ is controlled in norm by e_j, $j = k - m_k, \ldots, k$, for the depth m algorithm so long as the coefficients from the optimization remain bounded. In the results of section 4, the residual w_k is shown to converge to zero under Assumption 3.2. This is sufficient to establish convergence of the error $x_k - x^*$ to zero as

$$\|x_k - x^*\| \le \|x_k - g(x_k)\| + \|g(x_k) - g(x^*)\| \le \|w_{k+1}\| + \kappa \|x_k - x^*\|,$$

by which $\|x_k - x^*\| \le (1-\kappa)^{-1} \|w_{k+1}\|$.

3.1. Expansion of the residual. Based on Assumption 3.1 the error term $\tilde{e}_{k+1}$ of (2.4) has a Taylor expansion

$$\tilde{e}_{k+1} \coloneqq g(x_k) - g(x_{k-1}) = \int_0^1 g'(z_k(t); e_k) \, \mathrm{d}\, t, \tag{3.1}$$

where $z_k(t) = x_{k-1} + te_k$. Using (3.1) we next derive an expansion of the residual w_{k+1} in terms of the differences of consecutive iterates $e_k, \ldots, e_{k-m_{k-1}}$. We start with the definition of the residual by (2.4) and the expansion of iterate x_k by the update (2.5),

$$w_{k+1} = g(x_k) - x_k = (1 - \beta_{k-1})(g(x_k) - x_{k-1}^{\alpha}) + \beta_{k-1}(g(x_k) - \tilde{x}_k^{\alpha}). \tag{3.2}$$

Expanding the first term on the right-hand side of (3.2) yields

$$\begin{aligned} g(x_k) - x_{k-1}^{\alpha} &= \sum_{j=k-m_{k-1}-1}^{k-1} \alpha_j^k (g(x_k) - x_j) \\ &= \sum_{j=k-m_{k-1}-1}^{k-1} \alpha_j^k (g(x_j) - x_j) \\ &\quad + \sum_{j=k-m_{k-1}}^{k} \left(\sum_{n=k-m_{k-1}-1}^{j-1} \alpha_n^k \right) (g(x_j) - g(x_{j-1})) \\ &= w_k^{\alpha} + \sum_{j=k-m_{k-1}}^{k} \gamma_j \tilde{e}_{j+1}, \end{aligned} \tag{3.3}$$

where

$$\gamma_j := \sum_{n=k-m_{k-1}-1}^{j-1} \alpha_n^k. \tag{3.4}$$

It is worth noting that $\gamma_k = 1$. Expanding the second term on the right-hand side of (3.2), we get

$$g(x_k) - \tilde{x}_k^{\alpha} = \sum_{j=k-m_{k-1}-1}^{k-1} \alpha_j^k (g(x_k) - g(x_j)) = \sum_{j=k-m_{k-1}}^{k} \gamma_j \tilde{e}_{j+1}. \tag{3.5}$$

Reassembling (3.2) with (3.3) and (3.5) followed by (3.1), we have

$$\begin{aligned} w_{k+1} &= (1-\beta_{k-1}) w_k^{\alpha} + \sum_{j=k-m_{k-1}}^{k} \gamma_j \tilde{e}_{j+1} \\ &= (1-\beta_{k-1}) w_k^{\alpha} + \sum_{j=k-m_{k-1}}^{k} \gamma_j \int_0^1 g'(z_j(t); e_j) \, \mathrm{d}\, t. \end{aligned} \tag{3.6}$$

We now take a closer look at the last term of (3.6). For each $j = k - m_{k-1}, \ldots, k-1$, adding and subtracting intermediate averages allows

$$\int_0^1 g'(z_j(t); e_j) \, \mathrm{d}\, t = \int_0^1 g'(z_k(t); e_j) \, \mathrm{d}\, t + \sum_{n=j}^{k-1} \int_0^1 g'(z_n(t); e_j) - g'(z_{n+1}(t); e_j) \, \mathrm{d}\, t. \tag{3.7}$$

Summing over the j's the sum on the right-hand side of (3.6) may be expressed as

$$\begin{aligned} \sum_{j=k-m_{k-1}}^{k} \gamma_j \int_0^1 g'(z_j(t); e_j) \, \mathrm{d}\, t &= \gamma_j \int_0^1 g' \left(z_k(t); \sum_{j=k-m_{k-1}}^{k} e_j \right) \mathrm{d}\, t \\ &\quad + \sum_{j=k-m_{k-1}}^{k-1} \sum_{n=j}^{k-1} \gamma_j \int_0^1 g'(z_n(t); e_j) - g'(z_{n+1}(t); e_j) \, \mathrm{d}\, t. \end{aligned} \tag{3.8}$$

The next calculation shows that $\sum_{j=k-m_{k-1}}^{k} \gamma_j e_j$ is equal to $\beta_{k-1} w_k^\alpha$. First, observe that $\gamma_j - \gamma_{j-1} = \alpha_{j-1}^k$ and $\gamma_{k-m_{k-1}} = \alpha_{k-m_{k-1}-1}^k$. Separating the first term of the sum and using $\gamma_k = 1$,

$$\begin{aligned}\sum_{j=k-m_{k-1}}^{k} \gamma_j e_j &= x_k - x_{k-1} + \sum_{j=k-m_{k-1}}^{k-1} \gamma_j (x_j - x_{j-1}) \\ &= x_k - x_{k-1} + \gamma_{k-1} x_{k-1} - \sum_{j=k-m_{k-1}-1}^{k-2} \alpha_j^k x_j \\ &= x_k - \alpha_{k-1}^k x_{k-1} - \sum_{j=k-m_{k-1}-1}^{k-2} \alpha_j^k x_j = x_k - x_{k-1}^\alpha. \end{aligned} \tag{3.9}$$

From (3.9) and the decomposition of x_k in terms of update (2.2), we have that

$$\begin{aligned}\sum_{j=k-m_{k-1}}^{k} \gamma_j e_j = x_k - x_{k-1}^\alpha &= (1-\beta_{k-1}) x_{k-1}^\alpha + \beta_{k-1} \tilde{x}_k^\alpha - x_{k-1}^\alpha \\ &= \beta_{k-1} (\tilde{x}_k^\alpha - x_{k-1}^\alpha) = \beta_{k-1} w_k^\alpha. \end{aligned} \tag{3.10}$$

Putting (3.10) together with (3.8) and (3.6) then yields

$$\begin{aligned} w_{k+1} &= \int_0^1 (1-\beta_{k-1}) w_k^\alpha + \beta_{k-1} g'(z_k(t); w_k^\alpha) \, \mathrm{d}\, t \\ &\quad + \sum_{j=k-m_{k-1}}^{k-1} \sum_{n=j}^{k-1} \gamma_j \int_0^1 g'(z_n(t); e_j) - g'(z_{n+1}(t); e_j) \, \mathrm{d}\, t \\ &= \mathcal{L} + \mathcal{H}, \end{aligned} \tag{3.11}$$

where $\mathcal{L} = \int_0^1 (1-\beta_{k-1}) w_k^\alpha + \beta_{k-1} g'(z_k(t); w_k^\alpha) \, \mathrm{d}\, t$, so that $\mathcal{L}$ and $\mathcal{H}$ contain the respective lower- and higher-order parts of the decomposition. Taking norms in (3.11) and applying Assumption 3.1 followed by triangle inequalities to the terms inside the sums of $\mathcal{H}$ yields

$$\|\mathcal{L}\| \le ((1-\beta_{k-1}) + \kappa \beta_{k-1}) \, \|w_k^\alpha\| \,, \tag{3.12}$$

$$\begin{aligned} \|\mathcal{H}\| &\le \hat{\kappa} \sum_{j=k-m_{k-1}}^{k-1} |\gamma_j| \, \|e_j\| \sum_{n=j}^{k-1} \int_0^1 \|-t e_{n+1} - (1-t) e_n\| \, \mathrm{d}\, t \\ &\le \frac{\hat{\kappa}}{2} \sum_{j=k-m_{k-1}}^{k-1} |\gamma_j| \, \|e_j\| \sum_{n=j}^{k-1} (\|e_{n+1}\| + \|e_n\|) \,. \end{aligned} \tag{3.13}$$

Based on the expansion of w_{k+1} provided by (3.11) and the bounds (3.12)–(3.13) we now proceed to bound the higher-order terms to establish convergence of Algorithm 2.1 at an accelerated rate.

3.2. Relating the difference of consecutive iterates to residuals. We now derive estimates to bound (in norm) the e_j's from the right-hand side of (3.11) by the corresponding w_j's. The bounds in this subsection hold under Assumption 3.2, namely g is a contractive operator.

Under Assumption 3.2 we have the inequality

$$(1-\kappa)\,\|e_n\| \le \|e_n\| - \|\tilde{e}_{n+1}\| \le \|\tilde{e}_{n+1} - e_n\| = \|w_{n+1} - w_n\|\,. \tag{3.14}$$

The next lemma establishes a bound for e_{j-1} in terms of w_j and w_{j-1} in the case of depth $m = 1$. The subsequent lemma generalizes the same idea for general m.

LEMMA 3.3. *Under the conditions of Assumption* 3.2*, the following bounds hold:*

$$|\alpha^j_{j-1}|\,\|e_{j-1}\| \le \frac{1}{1-\kappa}\,\|w_{j-1}\|\,, \tag{3.15}$$

$$|\alpha^j_{j-2}|\,\|e_{j-1}\| \le \frac{1}{1-\kappa}\,\|w_j\|\,. \tag{3.16}$$

Proof. Begin by rewriting the optimization problem (2.1) in the equivalent form

$$\eta = \operatorname{argmin} \|w_{j-1} + \eta(w_j - w_{j-1})\|^2\,,$$

where $\alpha^j_{j-1} = \eta$ and $\alpha^j_{j-2} = 1 - \eta$. The critical point η then satisfies $\eta\,\|w_j - w_{j-1}\|^2 = (w_{j-1}, w_j - w_{j-1})$. Applying Cauchy–Schwarz and triangular inequalities yields $|\eta|\,\|w_j - w_{j-1}\| \le \|w_{j-1}\|$. Applying (3.14) with $n = j - 1$ yields the result (3.15).

Next, rewrite the optimization problem (2.1) in another equivalent form,

$$\gamma = \operatorname{argmin} \|w_j - \gamma(w_j - w_{j-1})\|^2\,, \tag{3.17}$$

where the equivalence follows with $\alpha^j_{j-2} = \gamma$ and $\alpha^j_{j-1} = 1 - \gamma$. Following the same procedure as above yields $|\gamma|\,\|w_j - w_{j-1}\| \le \|w_j\|$. Applying (3.14) at level $n-1$ then yields the second result (3.16). ∎

The use of γ as the second parameter in the proof above is not purely coincidental, as this γ agrees with $\gamma_{k-m_{k-1}}$ used in section 3.1 with $k = j$ and $m_{k-1} = 1$. The same essential technique yields the necessary bounds for $m \ge 2$. The estimate for general m is given in Lemma 3.4, with the particular estimate for $m = 2$ given as a proposition.

As in the $m = 1$ case above, two forms of the optimization problem are used. The γ-formulation is used to bound the terms $|\gamma_j|\,\|e_j\|$ that appear from the expansion (3.11); whereas, the η-formulation is used to bound the term $\|e_k\|$ as it appears in the numerator without leading optimization coefficients. It is then of particular importance that estimates of the form $c\,\|e_j\| \le \Sigma k_n\,\|w_n\|$ have the property that c is bounded away from zero. This is a reasonable assumption on the leading coefficient $c = \alpha^k_{k-1}$ for each k, as some nonvanishing component in the latest search direction is necessary for progress. The bounds below should be understood under the usual convention that the sums are zero if the lower index is greater than the upper.

LEMMA 3.4. *Under the conditions of Assumption* 3.2*, the following bounds hold:*

$$\|e_j\| \le \frac{1}{1-\kappa}\left(\|w_{j+1}\| + \|w_j\|\right), \tag{3.18}$$

$$|\alpha_{j-1}^j|\,\|e_{j-1}\| \le \frac{1}{1-\kappa}\left(|\eta_{j-1}|\,\|w_{j-1}\| + \sum_{n=j-m_{j-1}}^{j-2} |\alpha_{n-1}^j|\,\|w_n\|\right) \tag{3.19}$$

$$|\gamma_{p-1}|\,\|e_{p-1}\| \le \frac{1}{1-\kappa}\left(\sum_{n=j-m_{j-1}}^{p-2} |\alpha_{n-1}^j|\,\|w_n\| + |\gamma_{p-2}|\,\|w_{p-1}\| + |\gamma_p|\,\|w_p\|\right.$$

$$\left. + \sum_{n=p+1}^{j} |\alpha_{n-1}^j|\,\|w_n\|\right). \tag{3.20}$$

with $\eta_{j-1} = \alpha_{j-1}^j + \alpha_{j-2}^j$ *as in* (3.21)*, and* γ_p,γ_{p-1},γ_{p-2}*, given below by* (3.22)*.*

As discussed above, each bound plays a different role in the final result. The first, (3.18), is used for any $\|e_j\|$ with $j \le k-1$ that does not appear multiplied by a corresponding coefficient $|\gamma_j|$. The second, (3.19), is used to bound $\|e_k\|$. The third, (3.20), is used to bound terms of the form $|\gamma_{p-1}|\,\|e_{p-1}\|$, as appearing in each outer sum of (3.13). Relating these estimates to the $m_{k-1} = 1$ case of Lemma 3.3, (3.19) reduces to (3.15) and (3.20) with $p = j$ reduces to (3.16), noting from (3.22) that $\gamma_{j-1} = \alpha_{j-2}^j$ and $\gamma_j = \alpha_{j-2}^j + \alpha_{j-1}^j = 1$.

Proof. The first bound (3.18) follows directly from (3.14) and a triangle inequality. For the second two bounds, we recall the optimization problem (2.1) at level j is to minimize

$$\left\| \sum_{n=j-m_{j-1}-1}^{j-1} \alpha_n^j w_{n+1} \right\| \quad \text{subject to} \quad \sum_{n=j-m_{j-1}-1}^{j-1} \alpha_n^j = 1.$$

Differencing from the left and right, respectively, this can be posed as the following unconstrained optimization problems:

$$\text{minimize} \left\| w_{j-m_{j-1}} + \sum_{n=j-m_{j-1}+1}^{j} \eta_n (w_n - w_{n-1}) \right\|^2, \quad \eta_n = \sum_{i=n-1}^{j-1} \alpha_i^j, \tag{3.21}$$

$$\text{minimize} \left\| w_j - \sum_{n=j-m_{j-1}+1}^{j} \gamma_{n-1} (w_n - w_{n-1}) \right\|^2, \qquad \gamma_n = \sum_{i=j-m_{j-1}-1}^{n-1} \alpha_i^j. \tag{3.22}$$

Note that (3.22) coincides with (3.4), which agrees with the unconstrained form of the optimization problem in, for instance, [8]. To help reduce notation, denote $m = m_{j-1}$ for the remainder of the proof.

Starting with estimate (3.19) we are concerned with bounding-in-norm the leading difference term $w_j - w_{j-1}$. Expanding the norm squared (3.21) as an inner product and seeking the critical point for η_j yields

$$\eta_j \|w_j - w_{j-1}\|^2 + (w_j - w_{j-1}, w_{j-m}) + \sum_{n=j-m+1}^{j-1} \eta_n (w_j - w_{j-1}, w_n - w_{n-1}) = 0.$$

Recombining the terms inside the sum, noting $\eta_{n-1} - \eta_n = \alpha^j_{n-2}$ and $\eta_j = \alpha^j_{j-1}$, we obtain

$$\alpha^j_{j-1} \|w_j - w_{j-1}\|^2 = -(\alpha^j_{j-1} + \alpha^j_{j-2})(w_j - w_{j-1}, w_{j-1}) - \sum_{n=j-m}^{j-2} \alpha^j_{n-1}(w_j - w_{j-1}, w_n).$$

Applying Cauchy–Schwarz and triangle inequalities then yields

$$|\alpha^j_{j-1}| \|w_j - w_{j-1}\| \le |\alpha^j_{j-1} + \alpha^j_{j-2}| \|w_{j-1}\| + \sum_{n=j-m}^{j-2} \alpha^j_{n-1} \|w_n\|.$$

Applying (3.14), the result (3.19) follows.

Similarly for (3.20), expanding the norm of (3.22) as an inner product and seeking the critical point for each γ_{p-1} yields

$$\gamma_{p-1} \|w_p - w_{p-1}\|^2 = (w_p - w_{p-1}, w_j) - \sum_{n=j-m+1, n\neq p}^{j} \gamma_{n-1}(w_p - w_{p-1}, w_n - w_{n-1}).$$

Recombining the terms inside the sum using $\gamma_n - \gamma_{n-1} = \alpha^j_{n-1}$ and $\gamma_{j-m} = \alpha^j_{j-m-1}$, we obtain

$$\begin{aligned}\gamma_{p-1} \|w_p - w_{p-1}\|^2 = &\sum_{n=j-m}^{p-2} \alpha^j_{n-1}(w_p - w_{p-1}, w_n) - \gamma_{p-2}(w_p - w_{p-1}, w_{p-1}) \\ &+ \gamma_p(w_p - w_{p-1}, w_p) \\ &+ \sum_{n=p+1}^{j} \alpha^j_{n-1}(w_p - w_{p-1}, w_n).\end{aligned}$$

Applying now Cauchy–Schwarz and triangle inequalities,

$$\begin{aligned}|\gamma_{p-1}| \|w_p - w_{p-1}\| \le &\sum_{n=j-m}^{p-2} |\alpha^j_{n-1}| \|w_n\| + |\gamma_{p-2}| \|w_{p-1}\| + |\gamma_p| \|w_p\| \\ &+ \sum_{n=p+1}^{j} |\alpha^j_{n-1}| \|w_n\|.\end{aligned}$$

Applying (3.14), the result (3.20) follows. ∎

For the convenience of subsequent calculations, the bounds (3.21) and (3.22) used to bound $\|w_{k+1}\|$ for the case of depth $m = 2$ are summarized in the following proposition.

PROPOSITION 3.5 (depth $m = 2$). *With depth $m = 2$ the estimates* (3.19) *and* (3.20) *reduce to*

$$\|e_{j-1}\| \le \frac{1}{1-\kappa} \left(\|w_j\| + \|w_{j-1}\|\right), \tag{3.23}$$

$$|\alpha^{k+1}_k| \|e_k\| \le \frac{1}{1-\kappa} \left(|\alpha^{k+1}_k + \alpha^{k+1}_{k-1}| \|w_k\| + |\alpha^{k+1}_{k-2}| \|w_{k-1}\|\right), \tag{3.24}$$

$$|\gamma_{j-1}| \|e_{j-1}\| \le \frac{1}{1-\kappa} \left(\|w_j\| + |\alpha^j_{j-3}| \|w_{j-1}\| + |\alpha^j_{j-3}| \|w_{j-2}\|\right), \tag{3.25}$$

$$|\gamma_{j-2}| \|e_{j-2}\| \le \frac{1}{1-\kappa} \left(|\alpha^j_{j-1}| \|w_j\| + |1 - \alpha^j_{j-1}| \|w_{j-1}\|\right). \tag{3.26}$$

The second two bounds (3.25) and (3.26) follow from (3.20) noting from (3.22), that for $m = 2$ we have $\gamma_{j-2} = \alpha^j_{j-3}$, $\gamma_{j-1} = 1 - \alpha^j_{j-1}$ and $\gamma_j = 1$.

3.3. Explicit computation of the optimization gain. The stage-k gain θ_k has a simple description assuming the optimization is performed over a norm $\|\cdot\|$ induced by an inner product $(\cdot, \cdot)$, in other words in a Hilbert space setting.

Consider the unconstrained γ-form of the optimization problem (3.22) at iteration k with depth m: Find $\gamma_{k-m+1}, \ldots, \gamma_k$ that minimize

$$\left\| w_{k+1} - \sum_{n=k-m+1}^{k} \gamma_n (w_{n+1} - w_n) \right\|^2 = \left\| w_{k+1} - F^k \gamma^k \right\|^2, \tag{3.27}$$

where F^k is the matrix with columns $w_{n+1} - w_n$, $n = k - m + 1, \ldots, k$, and γ^k is the corresponding vector of coefficients $\gamma_{k-m+1}, \ldots, \gamma_k$. Indeed, (3.27) (or equivalently reindexed) is the preferred way to state the optimization problem [21], particularly in the case where $\|\cdot\|$ is the l_2 norm and a fast QR algorithm can be used.

This is also the preferred statement of the problem to understand the gain θ_{k+1} from (2.6), which satisfies $\left\|w^\alpha_{k+1}\right\| = \theta_{k+1} \|w_{k+1}\|$. Define the unique decomposition $w_{k+1} = w_R + w_N$ with $w_R \in \text{Range}\,(F^k)$ and $w_N \in \text{Null}\,((F^k)^T)$. Then w_N is the least-squares residual satisfying $\|w_N\| = \left\|w_{k+1} - F^k\gamma^k\right\| = \left\|w^\alpha_{k+1}\right\| = \theta_{k+1}\|w_{k+1}\|$ meaning

$$\theta_{k+1} = \sqrt{1 - \frac{\|w_R\|^2}{\|w_{k+1}\|^2}}, \tag{3.28}$$

and, θ_{k+1} has the interpretation of the direction-sine between w_{k+1} and the subspace spanned by $\{w_{n+1} - w_n\}_{n=k-m+1}^k$. This is particularly clear in the case $m = 1$, where solving for the critical point γ of (3.17) yields

$$\gamma = \frac{(w_{k+1}, w_{k+1} - w_k)}{\|w_{k+1} - w_k\|^2}.$$

Expanding $\theta^2_{k+1}\|w_{k+1}\|^2 = \|w_{k+1} - \gamma(w_{k+1} - w_k)\|^2$ and using the particular value of γ above yields

$$1 - \theta^2_{k+1} = \frac{(w_{k+1}, w_{k+1} - w_k)^2}{\|w_{k+1} - w_k\|^2 \|w_{k+1}\|^2},$$

with the clear interpretation that $(1 - \theta^2_{k+1})^{1/2}$ is the direction cosine between w_{k+1} and $w_{k+1} - w_k$; hence θ_{k+1} is the direction-sine.

If, indeed, an (economy) QR algorithm $F^k = Q_1 R_1$ is used to solve the optimization problem, then $\theta_{k+1} = \sqrt{1 - (\left\|Q_1^T w_{k+1}\right\| / \|w_{k+1}\|)^2}$, which can be used to predict whether an accelerated step would be (sufficiently) beneficial. This explicit computation of θ_{k+1} is used in section 5.2 to propose an adaptive damping strategy based on the gain at each step. Finally, it is noted that the improvement in the gain θ_{k+1} as m is increased depends on sufficient linear independence or small direction cosines between the columns of F^k, as information from earlier in the history is added. This is discussed in some greater depth in [21].

4. Convergence rates. We next analyze convergence rates for depths $m = 1$ and $m = 2$, followed by the corresponding analysis for general m. The two simpler cases are included as they show how the analysis fits together with less technicality.

4.1. Convergence rates for depths $m = 1$ and $m = 2$. First, we put the expansion (3.11) together with the bounds (3.15)–(3.16) for a convergence proof for the simplest case of $m = 1$.

THEOREM 4.1 (convergence of the residual with depth $m = 1$). *On the satisfaction of Assumptions* 3.1 *and* 3.2*, if the coefficients $\alpha_k^{k+1}, \alpha_{k-1}^k$ remain bounded and bounded away from zero, the following bound holds for the residual w_{k+1} from Algorithm* 2.1 *with depth $m = 1$:*

$$\|w_{k+1}\| \leq \theta_k((1-\beta_{k-1}) + \kappa\beta_{k-1}) \|w_k\| + \mathcal{O}\left(\|w_k\|^2\right) + \mathcal{O}\left(\|w_{k-1}\|^2\right).$$

Remark 4.2. The assumptions on the coefficients α_j^k arising from the optimization problem are similar to those of [20]. These assumptions could be eliminated by solving instead a constrained optimization problem that enforces boundedness of the parameters, resulting in a modified gain $\hat{\theta}_k$ which satisfies $\theta_k \leq \hat{\theta}_k \leq 1$. This, along with two other options for enforcing boundedness of the optimization coefficients, can be found in [20, section 2.2].

Proof. In this case the expansion found for $\|w_{k+1}\|$ in (3.11)–(3.13) reduces to

$$\|w_{k+1}\| \leq \theta_k((1-\beta_{k-1}) + \kappa\beta_{k-1}) \|w_k\| + \frac{\hat{\kappa}}{2}(\|e_k\| + \|e_{k-1}\|)|\gamma_{k-1}| \|e_{k-1}\|. \tag{4.1}$$

The preceding bound (4.1) holds regardless of whether g is globally contractive (Assumption 3.2); hence for error terms $\|e_k\|$ and $\|e_{k-1}\|$ small enough, contraction of the error may be observed depending on the search direction, particularly if a damping factor $0 < \beta < 1$ is applied, and if the gain θ_k is sufficiently less than one. This justifies the observation that Anderson acceleration can enlarge the effective domain of convergence of a fixed-point iteration.

For the remainder of the calculation, we consider the case of a contractive operator, meaning Assumption 3.2 is satisfied. Applying (3.16) with $j = k$ to the $|\gamma_{k-1}| \|e_{k-1}\|$, recalling by (3.4) we have $\gamma_{k-1} = \alpha_{k-2}^k$; and applying (3.15) with $j = k+1$ and $j = k$, respectively, to the remaining $\|e_k\|$ and $\|e_{k-1}\|$ allows

$$\begin{aligned}\|w_{k+1}\| &\leq \theta_k((1-\beta_{k-1}) + \kappa\beta_{k-1}) \|w_k\| + \frac{\hat{\kappa}}{2(1-\kappa)^2}\left(\frac{\|w_k\|}{\alpha_k^{k+1}} + \frac{\|w_{k-1}\|}{\alpha_{k-1}^k}\right)\|w_k\| \\ &= \theta_k((1-\beta_{k-1}) + \kappa\beta_{k-1}) \|w_k\| + \mathcal{O}\left(\|w_k\|^2\right) + \mathcal{O}\left(\|w_{k-1}\|^2\right). \end{aligned} \tag{4.2}$$

∎

As discussed in section 3.2, α_k^{k+1} and α_{k-1}^k are each the leading coefficients in their respective optimization problems, multiplying the most recent iterate. As such, these coefficients may be reasonably considered to be bounded away from zero.

The case of $m = 2$ follows similarly, combining (3.11) with (3.24)–(3.26). Here we make explicit use of the decomposition $w_{k+1} = \mathcal{L} + \mathcal{H}$.

THEOREM 4.3 (convergence of the residual with depth $m = 2$). *On the satisfaction of Assumptions* 3.1 *and* 3.2*, if the coefficients $\alpha_{j-3}^j, \alpha_{j-2}^j$, $j = k, k+1$ remain bounded, and α_k^{k+1} remains bounded away from zero, the following bound holds for the residual w_{k+1} from Algorithm* 2.1 *with depth $m = 2$:*

$$\begin{aligned}\|w_{k+1}\| \leq \theta_k((1-\beta_{k-1}) + \kappa\beta_{k-1}) \|w_k\| &+ \mathcal{O}\left(\|w_k\|^2\right) \\ &+ \mathcal{O}\left(\|w_{k-1}\|^2\right) + \mathcal{O}\left(\|w_{k-2}\|^2\right).\end{aligned} \tag{4.3}$$

Proof. For depth $m = 2$ the residual expansion (3.11)–(3.13) reduces to

(4.4)
$$\|w_{k+1}\| \leq \|\mathcal{L}\| + \|\mathcal{H}\|,$$

(4.5)
$$\|\mathcal{L}\| \leq \theta_k((1-\beta_{k-1}) + \kappa\beta_{k-1}) \|w_k\|,$$

(4.6)
$$\|\mathcal{H}\| \leq \frac{\hat{\kappa}}{2}(\|e_k\| + \|e_{k-1}\|)|\gamma_{k-1}| \|e_{k-1}\| + \hat{\kappa}(\|e_{k-2}\| + 2\|e_{k-1}\| + \|e_k\|)|\gamma_{k-2}| \|e_{k-2}\|.$$

Applying (3.25) and (3.26) to (4.6) yields

$$\begin{aligned}\|\mathcal{H}\| &\leq \frac{\hat{\kappa}}{2(1-\kappa)}(\|e_k\| + \|e_{k-1}\|)\left(\|w_k\| + |\alpha_{k-3}^k| \|w_{k-1}\| + |\alpha_{k-3}^k| \|w_{k-2}\|\right) \\ &+ \frac{\hat{\kappa}}{2(1-\kappa)}(\|e_k\| + 2\|e_{k-1}\| + \|e_{k-2}\|)\left(|\alpha_{k-1}^k| \|w_k\| + |1-\alpha_{k-1}^k| \|w_{k-1}\|\right). \end{aligned} \tag{4.7}$$

Applying (3.24) to $\|e_k\|$ and (3.23) to $\|e_{k-1}\|$ in (4.7) then yields

$$\begin{aligned}\|\mathcal{H}\| \leq{}& \frac{\hat{\kappa}}{2(1-\kappa)^2}\left(\|w_k\| + \|w_{k-1}\| + \frac{1}{|\alpha_k^{k+1}|}\left(|\alpha_k^{k+1} + \alpha_{k-1}^{k+1}| \|w_k\| + |\alpha_{k-2}^{k+1}| \|w_{k-1}\|\right)\right) \\ &\times \left(\|w_k\| + |\alpha_{k-3}^k| \|w_{k-1}\| + |\alpha_{k-3}^k| \|w_{k-2}\|\right) \\ &+ \frac{\hat{\kappa}}{2(1-\kappa)^2}\Bigg(2\|w_k\| + 3\|w_{k-1}\| + \|w_{k-2}\| \\ &+ \frac{1}{|\alpha_k^{k+1}|}\left(|\alpha_k^{k+1} + \alpha_{k-1}^{k+1}| \|w_k\| + |\alpha_{k-2}^{k+1}| \|w_{k-1}\|\right)\Bigg) \\ &\times \left(|\alpha_{k-1}^k| \|w_k\| + |1-\alpha_{k-1}^k| \|w_{k-1}\|\right) \\ ={}& \mathcal{O}\left(\|w_k\|^2\right) + \mathcal{O}\left(\|w_{k-1}\|^2\right) + \mathcal{O}\left(\|w_{k-2}\|^2\right), \end{aligned} \tag{4.8}$$

where each term has bounded coefficients under the hypotheses of the theorem. Putting together (4.8) with (4.4) and (4.5) yields the result (4.3). ∎

4.2. Convergence rates for depth $m > 2$. Finally, we consider the result for general m.

THEOREM 4.4. *On the satisfaction of Assumptions* 3.1 *and* 3.2*, if the coefficients* $\alpha_{k-m-1}^j, \ldots, \alpha_{j-2}^j$, $j = k, k+1$*, remain bounded, and* α_k^{k+1} *remains bounded away from zero, the following bound holds for the residual* w_{k+1} *from Algorithm* 2.1 *with depth* $m > 2$*, assuming* $k > m$*:*

$$\|w_{k+1}\| \leq \theta_k((1-\beta_{k-1}) + \kappa\beta_{k-1}) \|w_k\| + \sum_{j=0}^{m} \mathcal{O}\left(\|w_{k-j}\|^2\right). \tag{4.9}$$

Remark 4.5. Using the same damping factor and without acceleration, the residual norm at step $k+1$ would be bounded by $((1-\beta_{k-1}) + \beta_{k-1}\kappa)\|w_k\|$. With acceleration, Theorem 4.4 demonstrates that $\|w_{k+1}\|$ is bounded by $\theta_k((1-\beta_{k-1}) + \beta_{k-1}\kappa)\|w_k\|$, plus an additional higher-order contribution $\sum_{j=0}^m \mathcal{O}\left(\|w_{k-j}\|^2\right)$. Hence, so long as this additional error does not offset the gain from the first-order term, improvement in convergence from Anderson acceleration will be attained.

Proof. We proceed by a direct argument on the lower-order terms and an inductive argument on the higher-order terms. From (3.11) we have $w_{k+1} = \mathcal{L} + \mathcal{H}$, where $\mathcal{L} \coloneqq \int_0^1 (1-\beta_{k-1}) w_k^\alpha + \beta_{k-1} g'(z_k(t); w_k^\alpha)\, \mathrm{d}\, t$.

For $k > m$, the depth is constant, $m_j = m$, $j \geq k-1$. Now define

$$\mathcal{H}^{(q)} \coloneqq \sum_{j=k-q}^{k-1} \sum_{n=j}^{k-1} \gamma_j \int_0^1 g'(z_n(t); e_j) - g'(z_{n+1}(t); e_j)\, \mathrm{d}\, t,\ 1 \leq q \leq m. \tag{4.10}$$

Then $\mathcal{H}^{(m)} = \mathcal{H}$ from (3.11), and $\|w_{k+1}\| \leq \|\mathcal{L}\| + \left\|\mathcal{H}^{(m)}\right\|$. To bound the lower-order part we have from (3.12) and (2.6) that

$$\|\mathcal{L}\| \leq \theta_k \left((1-\beta_{k-1}) + \kappa\beta_{k-1}\right) \|w_k\|. \tag{4.11}$$

Proceeding with the inductive part of the argument, we seek to show $\left\|\mathcal{H}^{(m)}\right\| \leq \sum_{j=0}^m \mathcal{O}\left(\|w_{k-j}\|^2\right)$. For the base step, consider $q = 1$. From (4.10), we have $\mathcal{H}^{(1)} = \int_0^1 g'(z_{k-1}(t); \gamma_{k-1} e_{k-1}) - g'(z_k(t); \gamma_{k-1} e_{k-1})\, \mathrm{d}\, t$, and

$$\left\|\mathcal{H}^{(1)}\right\| \leq \frac{\hat{\kappa}}{2} |\gamma_{k-1}| \, \|e_{k-1}\| \left(\|e_k\| + \|e_{k-1}\|\right). \tag{4.12}$$

While this looks similar to the expression in (4.1) from the $m = 1$ proof, here γ_{k-1} is a coefficient from the depth-m rather than the depth-1 algorithm. Expanding $|\gamma_{k-1}| \, \|e_{k-1}\|$ by (3.20) with $p = j = k$, $\|e_k\|$ by (3.19) with $j = k+1$, and $\|e_{k-1}\|$ by (3.18) with $j = k-1$ yields

$$\begin{aligned}
\left\|\mathcal{H}^{(1)}\right\| &\leq \frac{\hat{\kappa}}{2(1-\kappa)^2} \left(\sum_{n=k-m}^{k-2} |\alpha_{n-1}^k| \, \|w_n\| + |\gamma_{k-2}| \, \|w_{k-1}\| + |\gamma_k| \, \|w_k\| \right) \\
&\quad \times \left(\frac{|\eta_k|}{|\alpha_k^{k+1}|} \|w_k\| + \frac{1}{|\alpha_k^{k+1}|} \sum_{n=k-m+1}^{k-1} |\alpha_{n-1}^{k+1}| \, \|w_n\| + \|w_k\| + \|w_{k-1}\| \right) \\
&= \sum_{j=0}^m \mathcal{O}\left(\|w_{k-j}\|^2\right). \qquad (4.13)
\end{aligned}$$

From the hypotheses of the theorem, and $\eta_k = \alpha_k^{k+1} + \alpha_{k-1}^{k+1}$ from (3.21) with $n = k$ and $j = k+1$, each coefficient in (4.13) is bounded, by which the base step of the induction is satisfied. Assume now for each $l = 1, \ldots, q-1$, for $q \leq m$, the inductive hypothesis

$$\left\|\mathcal{H}^{(l)}\right\| \leq \sum_{j=0}^m \mathcal{O}\left(\|w_{k-j}\|^2\right). \tag{4.14}$$

Proceed with the inductive step, for $q \leq m$. From (4.10) we have

$$\begin{aligned}
\mathcal{H}^{(q)} &= \sum_{j=k-(q-1)}^{k-1} \sum_{n=j}^{k-1} \gamma_j \int_0^1 g'(z_n(t); e_j) - g'(z_{n+1}(t); e_j)\, \mathrm{d}\, t \\
&\quad + \gamma_{k-q} \sum_{n=k-q}^{k-1} \int_0^1 g'(z_n(t); e_{k-q}) - g'(z_{n+1}(t); e_{k-q})\, \mathrm{d}\, t \\
&= \mathcal{H}^{(q-1)} + \gamma_{k-q} \sum_{n=k-q}^{k-1} \int_0^1 g'(z_n(t); e_{k-q}) - g'(z_{n+1}(t); e_{k-q})\, \mathrm{d}\, t.
\end{aligned}$$

Taking norms and applying Assumption 3.1 as in (3.13) allows

$$\left\|\mathcal{H}^{(q)}\right\| \le \left\|\mathcal{H}^{(q-1)}\right\| + \frac{\hat{\kappa}}{2}|\gamma_{k-q}|\,\|e_{k-q}\| \sum_{n=k-q}^{k-1} (\|e_{n+1}\| + \|e_n\|)$$

$$\le \left\|\mathcal{H}^{(q-1)}\right\| + \frac{\hat{\kappa}}{2}|\gamma_{k-q}|\,\|e_{k-q}\| \left(\|e_k\| + 2\left(\sum_{n=k-q+1}^{k-1} \|e_n\| \right) + \|e_{k-q}\| \right). \tag{4.15}$$

Now $|\gamma_{k-q}|\,\|e_{k-q}\|$ can be bounded by (3.20) with $j = k$, and $\|e_k\|$ can be bounded by (3.19) exactly as it is in (4.13). The remaining terms can be bounded by (3.18). Specifically,

$$|\gamma_{k-q}|\,\|e_{k-q}\| \le \frac{1}{1-\kappa}\Bigg(|\gamma_{k-q+1}|\,\|w_{k-q+1}\| + |\gamma_{k-q-1}|\,\|w_{k-q}\| + \sum_{n=k-m}^{k-q-1} |\alpha_{n-1}^{k}|\,\|w_n\| + \sum_{n=k-q+2}^{k} |\alpha_{n-1}^{k}|\|w_n\| \Bigg), \tag{4.16}$$

where from (3.22), the coefficient $\gamma_{k-q+1} = \sum_{i=k-m-1}^{k-q} \alpha_i^k$, and $\gamma_{k-q-1} = \sum_{i=k-m-1}^{k-q-2} \alpha_i^k$, which is zero for $k = m$. The last sum in (4.16) is either zero for $q > 2$ or $|\alpha_{k-1}^k|\|w_k\|$ for $q = 2$. From (3.18) we have

$$2\left(\sum_{n=k-q+1}^{k-1} \|e_n\| \right) + \|e_{k-q}\| \le \frac{1}{1-\kappa}\left(2\,\|w_k\| + 4\left(\sum_{n=k-q+1}^{k-1} \|w_n\| \right) + 3\,\|w_{k-q+1}\| + \|w_{k-q}\| \right). \tag{4.17}$$

Putting (4.16), (4.17), and (3.19) with $j - 1 = k$ together into (4.15) yields

$$\begin{aligned}\left\|\mathcal{H}^{(q)}\right\| \le{}& \left\|\mathcal{H}^{(q-1)}\right\| \\ &+ \frac{\hat{\kappa}}{2(1-\kappa)^2}\Bigg(|\gamma_{k-q+1}|\,\|w_{k-q+1}\| + |\gamma_{k-q-1}|\,\|w_{k-q}\| \\ &+ \sum_{n=k-m}^{k-q-1} |\alpha_{n-1}^{k}|\,\|w_n\| + \sum_{n=k-q+2}^{k} |\alpha_{n-1}^{k}|\|w_n\| \Bigg) \\ &\times \Bigg\{ 2\,\|w_k\| + \frac{|\eta_k|}{|\alpha_k^{k+1}|}\,\|w_k\| + \frac{1}{|\alpha_k^{k+1}|} \sum_{n=k-m+1}^{k-1} |\alpha_{n-1}^{k+1}|\,\|w_n\| + 4\left(\sum_{n=k-q+1}^{k-1} \|w_n\| \right) \\ &+ 3\,\|w_{k-q+1}\| + \|w_{k-q}\| \Bigg\} \\ ={}& \sum_{j=0}^{m} \mathcal{O}\left(\|w_{k-j}\|^2 \right). \end{aligned} \tag{4.18}$$

Together with the inductive hypotheses (4.14) and the boundedness of the optimization coefficients from the hypotheses of the theorem, this establishes the inductive result for $q = 2, \ldots, m$. Putting the inductive result on the higher-order terms with $q = m$ together with the direct result (4.11) on the lower-order terms establishes (4.9), the result of the theorem. ∎

As discussed in section 3.3, even as the higher-order terms accumulate, there may still be an advantage to some extent to considering greater depth m, due to the improved gain from the optimization problem.

5. Numerical tests. We now give results of several numerical tests that illustrate the theory above. In particular, we illustrate that Anderson can speed up linear convergence but slows down quadratic convergence. Additionally, although our theoretical results do not rigorously justify it, our tests will also show that Anderson acceleration can expand the domain of convergence. Results from [15], a numerical study on Richards' equation governing flow in partially saturated media, also show this, and, in particular, that Anderson accelerated Picard-like iterates converge over a wider range of material parameters than do the corresponding unaccelerated versions of Picard or damped Newton iterations. We display our results to provide additional numerical evidence. It is not our purpose in this section to show how well Anderson acceleration works on a wide variety of problems; for this, see the references in the introduction.

5.1. Numerical tests for steady incompressible Navier–Stokes equation. Here we present numerical experiments to show the improved convergence provided by Anderson acceleration for solving the steady incompressible Navier–Stokes equations (NSE). In particular, we will illustrate how Anderson can improve the linear convergence rate of Picard iterations and expand the domain of convergence for both Picard and Newton iterations, but how Anderson acceleration can lower the order of convergence in Newton iterations.

The NSE are given in a domain Ω by

$$u \cdot \nabla u + \nabla p - \nu \Delta u = f, \tag{5.1}$$

$$\nabla \cdot u = 0, \tag{5.2}$$

where ν is the kinematic viscosity, f is a forcing, u and p represent velocity and pressure, and the system must be equipped with appropriate boundary conditions. The $L^2(\Omega)$ norm and inner product will be denoted by $\|\cdot\|$ and $(\,\cdot\,,\,\cdot\,)$ in this subsection.

The tests we consider are for the two-dimensional lid-driven cavity problem, which uses a domain $\Omega = (0,1)^2$, no-slip ($u = 0$) boundary conditions on the sides and bottom, and a "moving lid" on top which is implemented by the Dirichlet boundary condition $u(x,1) = \langle 1, 0\rangle^T$. There is no forcing ($f = 0$), and the kinematic viscosity is set to be $\nu \coloneqq Re^{-1}$, where Re is the Reynolds number, and in our tests we use Re varying between 1000 and 10,000. Plots of the velocity streamlines for the steady NSE at $Re = 2500$ and 6000 are shown in Figure 5.1.

We discretize with $(X_h, Q_h) = ((P_2)^2, P_1)$ Taylor–Hood finite elements on a $\frac{1}{256}$ uniform triangular mesh that provides 592,387 total degrees of freedom, and for the initial guess we used $u_h^0 = 0$ but satisfying the boundary conditions. Define the trilinear form b^* by

$$b^*(u, v, w) := (u \cdot \nabla v, w) + \frac{1}{2}((\nabla \cdot u)v, w).$$

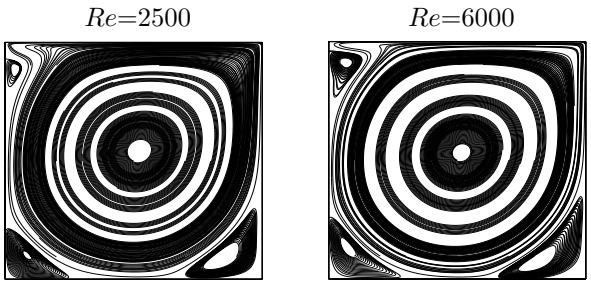

FIG. 5.1. *Streamline plots of the steady NSE driven cavity solutions with varying Re.*

The discrete steady incompressible NSE problem (with skew-symmetrized nonlinear term) reads as follows: Find $(u,p) \in (X_h, Q_h)$ satisfying for all $(v,q) \in (X_h, Q_h)$,

$$-(p, \nabla \cdot v) + \nu(\nabla u, \nabla v) + b^*(u,u,v) = (f,v), \tag{5.3}$$

$$(\nabla \cdot u, q) = 0. \tag{5.4}$$

Since this problem is nonlinear, we need a nonlinear solver. We consider two common nonlinear iterations, Picard and Newton, which are defined as follows.

ALGORITHM 5.1 (Picard iteration for steady NSE).
Step 1*: Choose* $u_0 \in X_h$.
Step k: Find $(u_k, p_k) \in (X_h, Q_h)$ *satisfying for all* $(v,q) \in (X_h, Q_h)$,

$$b^*(u_{k-1}, u_k, v) - (p_k, \nabla \cdot v) + \nu(\nabla u_k, \nabla v) = (f,v), \tag{5.5}$$

$$(\nabla \cdot u_k, q) = 0. \tag{5.6}$$

ALGORITHM 5.2 (Newton iteration for steady NSE).
Step 1*: Choose* $u_0 \in X_h$.
Step k: Find $(u_k, p_k) \in (X_h, Q_h)$ *satisfying for all* $(v,q) \in (X_h, Q_h)$,

(5.7)
$$b^*(u_{k-1}, u_k, v) + b^*(u_k, u_{k-1}, v) - b^*(u_{k-1}, u_{k-1}, v) - (p_k, \nabla \cdot v) + \nu(\nabla u_k, \nabla v) = (f,v),$$

$$(\nabla \cdot u_k, q) = 0. \tag{5.8}$$

For sufficiently small data, the steady NSE and these iterations are well posed [13]. Hence we can consider both the Picard and Newton iterations as fixed-point iterations $u_{k+1} = g(u_k)$, where g is a solution operator of (5.5)–(5.6) for Picard or (5.7)–(5.8) for Newton. In this way, we can apply Anderson acceleration to both methods. Below, we test both the Picard and Newton iterations with Anderson acceleration. The linear systems are solved with a sparse direct solver.

5.1.1. Results for Anderson accelerated Picard iterations. For Picard iterations, we observe in Figure 5.2 that Picard without Anderson acceleration is converging linearly (although slowly) for $Re = 2500$, but is not converging for $Re = 6000$. With Anderson acceleration, however, we observe the convergence is improved for $Re = 2500$, and for $Re = 6000$ Anderson acceleration allows convergence (in this sense Anderson acceleration improves the domain of convergence). Hence a significant improvement of $m = 1$ over $m = 0$ is observed in both cases, and further improvement is observed by increasing to $m = 3$.

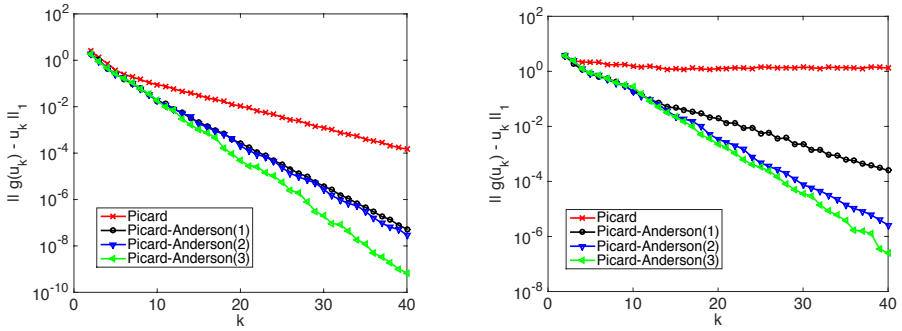

FIG. 5.2. *Convergence of the Anderson accelerated Picard iterations with* $Re = 2500$ *(left) and* $Re = 6000$ *(right).*

Box-plots of the θ_k's from the Picard iterations are shown in Figure 5.3. For $Re = 2500$ (left side), there is a clear decreasing trend in distribution of θ's as m increases, while for $Re = 6000$ the box-plots look rather similar but with $m = 1$ seemingly a little lower overall compared to $m = 2$. However, the lower values and outliers in these plots are critical, since one multiplication of a small factor takes many multiplications of larger factors to achieve the same residual decrease.

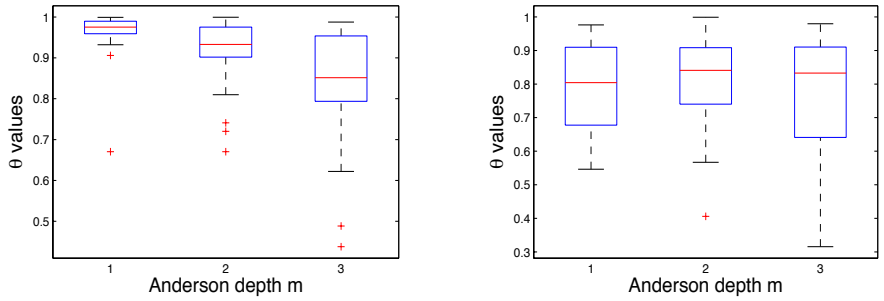

FIG. 5.3. *Box-plots of* θ *values for the Picard iterations with* $Re = 2500$ *(left) and* $Re = 6000$ *(right).*

As a final part of this test, we compare the number of iterations needed to converge the residual for the Picard iteration in the H^1 norm to a tolerance of 10^{-8}, for varying Re and varying m. Results are shown in Table 5.1, and again we observe a substantial improvement from Anderson acceleration. Even $m = 1$ is enough to provide convergence up to $Re = 10000$, although additional gain is made by increasing to $m = 2$ and to $m = 3$. It is interesting that convergence of the steady NSE is achieved for $Re = 9000$ and 10000 since the bifurcation point transition to transient flow is around 8000 [4]. F in Table 5.1 denotes failure in the table, which we define as not converging within 500 iterations (but we note that inspection of the last few iterations of each of these that failed indicates the iterations are nowhere near, or even approaching, convergence).

5.1.2. Results for Anderson accelerated Newton iterations. We next consider Anderson acceleration applied to Newton iterations for this same test problem, using $Re = 1000$ and $Re = 2500$. For the Newton iteration without Anderson acceleration, we ran with and without a line search (following the step 57 tutorial from

TABLE 5.1

Shown below are the number of Picard iterations needed to converge the nonlinear residual for the steady NSE up to 10^{-8} in the H^1 norm, for varying Re and m. F denotes a failure to reach convergence by 500 iterations.

Re / m	0	1	2	3
1000	36	32	29	26
2000	48	41	40	34
3000	86	49	45	37
4000	158	59	46	40
5000	363	55	48	44
6000	F	62	55	49
7000	F	65	61	53
8000	F	78	70	58
9000	F	94	83	68
10000	F	105	97	71

[5], and turning the line search off once the nonlinear residual reached 10^{-2}). For Newton with Anderson acceleration, we tested $m = 1,\ 2,\ 3$, without a line search (for $Re = 1000$, the results with and without a line search are the same). We used $u_h^0 = 0$ (and satisfying boundary conditions) as the initial guess, but also took two steps of Picard ($m = 0$) before beginning the Newton iterations.

Results are shown in Figure 5.4. For $Re = 1000$ (shown on the left) Newton converges quadratically without damping. The Newton–Anderson iterations with $m = 1, 2$, and 3 all display a lower (superlinear) order of convergence, which is particularly apparent toward the beginning of the iterative process. For $Re = 2500$ (shown on the right), Newton without a line search fails, and the remaining tests–Newton–Anderson with $m = 1, 2, 3$ and Newton with a line search–each show superlinear convergence. The observed convergence is not strictly monotonic in norm with respect to m, but is noticeably worse for $m = 3$ than for $m = 1$ or $m = 2$. The divergence for Newton without a line search demonstrates that the domain of convergence is expanded when Anderson acceleration is used, similar to the implemented line search.

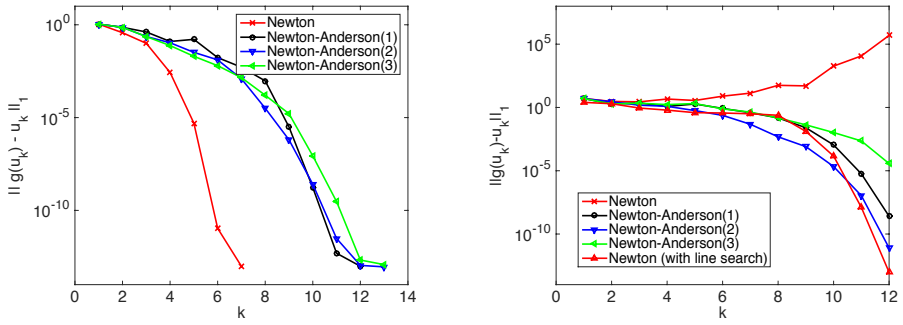

FIG. 5.4. *Convergence of the Anderson accelerated Newton iterations with Re = 1000 (left) and Re = 6000 (right).*

5.2. Numerical tests of Anderson accelerated and damped iterations applied to the *p*-Laplacian. As is well known, the damping (also called mixing) parameter β of Algorithm 2.1 may become important for convergence in the case of a fixed-point operator that is not contractive. The purpose of this test is to show how

explicit knowledge of the gain θ_{k+1} can be used to automatically choose a damping factor β_k to improve convergence stability and robustness with respect to depth m for noncontractive operators. The tests below show iterations converging well for depth $m < 2$, but at best with difficulty for $m > 2$, when $\beta_k = \beta$ is sufficiently small. For $\beta_k = \beta$ sufficiently large, the tests show efficient convergence for $m > 2$, no convergence for $m < 2$, and eventual but slow convergence for $m = 2$. Finally, when β_k is chosen by a simple heuristic strategy based on the gain θ_{k+1}, the iterations converge efficiently for each $m = 1, 2, 3, 4$.

We consider the p-Laplace equation, given in strong form by

$$-\operatorname{div}\left(\left(\frac{1}{2}|\nabla u|^2\right)^{(p-2)/2}\nabla u\right) = c, \tag{5.9}$$

with $c = 0.1$ and $p = 5$. For $p > 2$, (5.9) is a degenerate elliptic equation in which the nonlinear diffusion coefficient goes to zero as $|\nabla u|$ goes to zero, creating a challenging problem for nonlinear solvers. A regularized version, $-\operatorname{div}\left(\left(\varepsilon^2 + \frac{1}{2}|\nabla u|^2\right)^{(p-2)/2}\nabla u\right) = c$, with $\varepsilon = 10^{-5}$ and c, p as above, is used as a benchmark test in [7, section 6.5] on the composition of nonlinear solvers, comparing additive Schwarz and quasi-Newton methods with left and right preconditioning. We did not use the regularization term in our tests as it had little effect on the results.

The P_1 finite element approximation of (5.9) subject to homogeneous Dirichlet boundary conditions is the function $u \in V_h$ that satisfies

$$\int_\Omega \left(\frac{1}{2}|\nabla u|^2\right)^{(p-2)/2}\nabla u \cdot \nabla v \,\mathrm{d}\,x = \int_\Omega cv \,\mathrm{d}\,x \quad \text{for all} \quad v \in V_h, \tag{5.10}$$

where V_h is the space of continuous piecewise linear functions that vanish on the boundary. The simulations shown below were run on a 385×385 uniform left-crossed triangulation of $[0, 2] \times [0, 2]$ with 148,996 total degrees of freedom using a Python implementation of the FEniCS [1] finite element library. Each simulation was started from initial iterate $u_0 = xy(x-1)(y-1)(x-2)(y-2)$ (cf. [7]) and run to a residual tolerance of 10^{-7} in the l_2 norm, or stopped after a maximum number of iterations. The optimization problem is solved in the l_2 norm with an economy QR decomposition, and θ_k is computed as described in section 3.3. We consider accelerating the Picard iteration for this problem, defined as follows.

ALGORITHM 5.3 (Picard iteration for the p-Laplacian).
Step 1: Choose $u_0 \in V_h$.
Step k: Find $u_k \in V_h$ *satisfying for all* $v \in V_h$,

$$\int_\Omega \left(\frac{1}{2}|\nabla u_{k-1}|^2\right)^{(p-2)/2}\nabla u_k \cdot \nabla v \,\mathrm{d}\,x = \int_\Omega cv \,\mathrm{d}\,x. \tag{5.11}$$

The Picard iteration is not contractive, but does converge from the given initial iterate with a sufficiently small damping factor. In our tests, it converged in less than 100 iterations for a uniform choice of $\beta_k = \beta$ in the range $(0.13, 0.47)$. As seen by the expansion (3.11), the damping factor β_{k-1} explicitly alters the lower-order terms in the error expansion. If the solution operator for (5.11) is not contractive near the solution, then (3.12)–(3.13) still provides a bound for $\|w_{k+1}\|$ in terms of $\|w_k\|$ and higher-order terms involving differences of consecutive iterates $\|w_{k+1}\| \leq \theta_k(1 - \beta_{k-1} + \kappa\beta_{k-1})\|w_k\| + \mathcal{O}\big(\|e_k\|^2\big) + \cdots + \mathcal{O}\big(\|e_{k-m}\|^2\big)$. However, the bounds

(3.18)–(3.20) controlling the differences of consecutive iterates by residuals are no longer valid, so the theory is not complete.

Figure 5.5 on the left shows the convergence of the residuals for Picard and Picard–Anderson with $m = 1, 2, 3, 4$, with uniform damping factor $\beta_k = \beta = 0.2$. Shown here, the Picard iteration converges smoothly with $\beta = 0.2$, albeit with a slowing down of the convergence rate around iteration 35. The accelerated iterations with $m = 1$ and $m = 2$ show consecutive improvement. However, the $m = 3$ and $m = 4$ cases stagnate starting around iteration 40. From Figure 5.6 (left), the optimization gains θ_k overall improve after iteration 40, suggesting the higher-order terms, whose magnitude can be seen from Figure 5.5 (right) to vary between 10^{-2} and 1 over those iterations, are interfering with convergence. The iteration with $m = 4$ does eventually converge after 129 iterations. However, this example illustrates how a damping factor chosen too small can interfere with convergence for larger values of m.

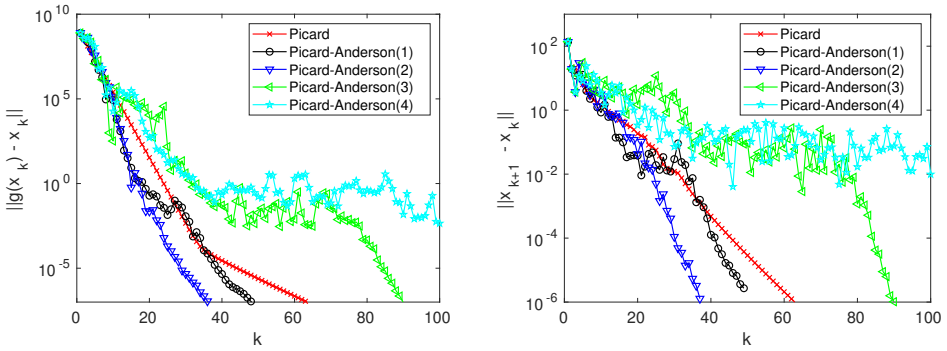

FIG. 5.5. *Convergence of the residuals $\|w_k\|$ (left) and difference of consecutive iterates $\|e_k\|$ (right) for damped iterations for the p-Laplace problem with damping parameter $\beta = 0.2$.*

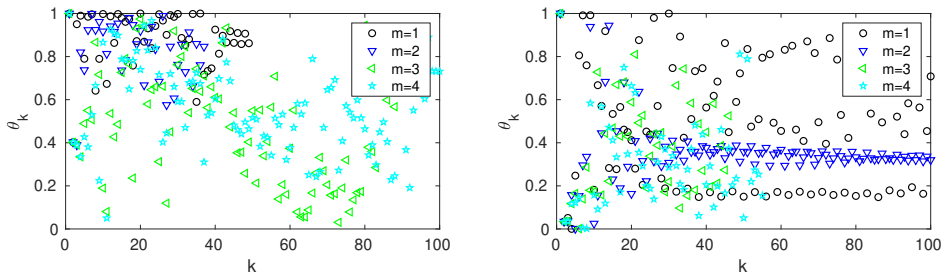

FIG. 5.6. *Optimization gains θ_k for damped iterations for the p-Laplace problem with damping parameter $\beta = 0.2$ (left) and $\beta = 0.75$ (right).*

In contrast, Figure 5.7 shows the history of residuals (left) with $\beta = 0.75$, well outside the regime where the Picard iteration converges. Indeed, the residual for the Picard iteration develops oscillatory behavior then stagnates around iteration 20, with the residual greater than one. The residual for $m = 1$ shows a more stable decrease at first, but it then also develops cyclic behavior, with $\|w_k\|$ stagnating just below the level of the Picard iteration. Anderson with $m = 2$ is more stable but also appears to stagnate with $\|e_k\| = \mathcal{O}(10^{-1})$ and $\|w_k\| = \mathcal{O}(10^{-2})$, and the corresponding gain

factors θ_k settling into a narrow band around 0.35 (Figure 5.6, right). Anderson with $m = 3$ and $m = 4$, however, both converge with an approximately linear rate.

It is useful to take a closer look at the borderline case $m = 2$, which as shown in Figure 5.7 (top right), does eventually converge in 230 iterations as $\|e_k\|^2$ drops below the level of $\|w_k\|$. Comparing the top and bottom right plots of Figure 5.7, while $\|w_k\|$ maintains its oscillatory behavior to the end, the oscillations in the gain θ_k subside by iteration 220 as the contribution from the higher-order terms diminishes. This example, with $\beta = 0.2$ and $\beta = 0.75$, illustrates that, while in agreement with results reported in [10, 19], the Picard–Anderson is more robust with respect to choice of the damping factor than Picard alone, a uniform damping factor may not be the most efficient choice, and the range of effective damping factors can depend on m. The adaptive strategy proposed next is illustrated here to reduce that dependence.

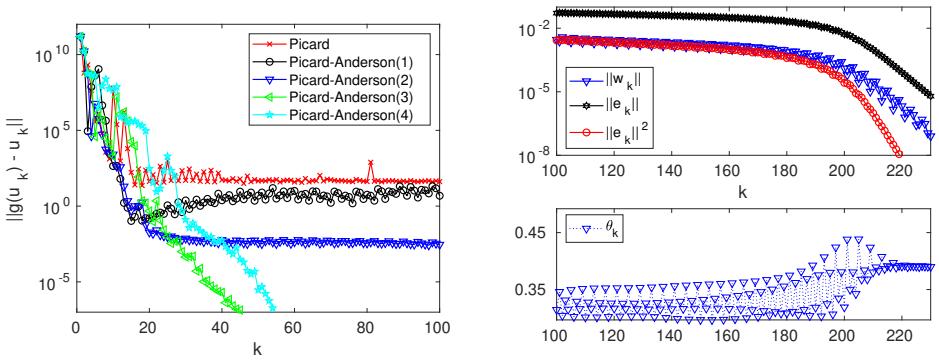

FIG. 5.7. *Left: Convergence of residuals* $\|w_k\|$ *for* $m = 1, 2, 3, 4$ *for damped iterations for the p-Laplace problem with damping parameter* $\beta = 0.75$. *Right: The last* 100 *iterations to convergence of residuals* $\|w_k\|$ *for* $m = 2$ *(top right), and corresponding gain factors* θ_k *(bottom right).*

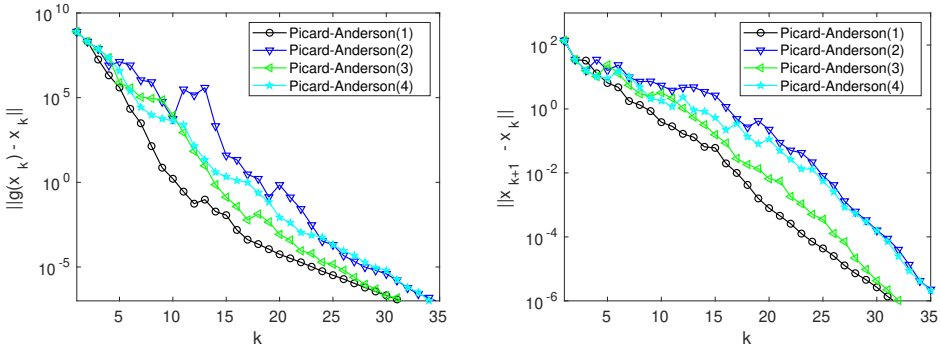

FIG. 5.8. *Convergence of residuals* $\|w_k\|$ *(left) and difference of consecutive iterates* $\|e_k\|$ *(right) for damped iterations for the p-Laplace problem with adaptively set damping parameter* $\beta_k = 0.9 - \theta_{k+1}/2$.

Finally, in Figure 5.8, results are shown with an adaptively set damping factor $\beta_k = 0.9 - \theta_{k+1}/2$, based on the gain θ_{k+1} computed as described in section 3.3. The heuristic choice of damping yields $0.4 \leq \beta_k \leq 0.9$, and leads to fewer iterations to convergence than with the uniform damping factors tested for each of $m = 1, 2, 3, 4$, without stagnation. In comparison with cases of $\beta = 0.2$ with $m = 3, 4$, and $\beta = 0.75$

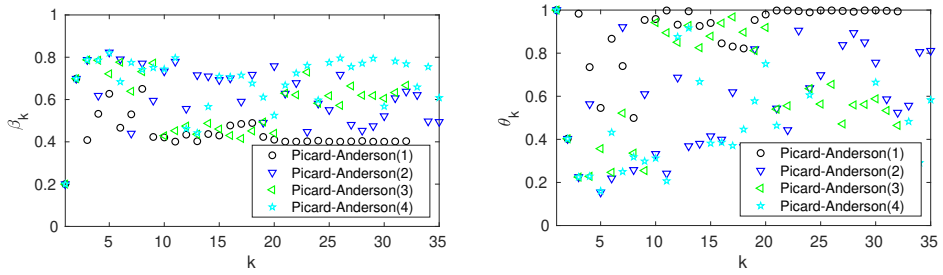

FIG. 5.9. *Damping factors* $\beta_k = 0.9 - \theta_k/2$ *(left), and optimization gains* θ_k *(right) corresponding to the error reduction shown in Figure* 5.8.

with $m = 1, 2$, this suggests using explicit knowledge of θ_{k+1} at each iteration to set β_k can help prevent the residual reduction from stalling.

The adaptively chosen damping factors β_k corresponding to optimization gains θ_k are shown in the left and right respective plots of Figure 5.9. For $m = 1$ the gains θ_k level off to nearly one between iterations 20 and 25, and convergence continues at a steady rate with a nearly constant damping factor of $\beta \approx 0.4$. For $m = 2, 3, 4$, the θ_k gains and β_k damping factors are more varied throughout the iteration. Notably the damping factor for $m = 2$ is above 0.75 for a good part of the first half of the simulation but takes lower values when higher values of the gain are encountered particularly towards the second half, which is apparently sufficient to stabilize the iteration. Unlike the results shown above in Figures 5.5 and 5.7, Picard–Anderson with $m = 1, 2, 3, 4$ all show similar convergence behavior using this damping strategy.

6. Conclusion. This paper shows for contractive fixed-point iterations how Anderson acceleration decreases the contribution to the total residual arising from first order terms; however, additional higher-order terms are introduced. In agreement with decades of experimental results, this shows that the method improves the first-order convergence rate for linearly converging fixed-point iterations in the vicinity of a fixed-point, in comparison to the fixed-point iteration run with the same damping factor. Our analysis reveals that the reduction in the contribution to the residual from the first-order terms depends at each step on the gain from the optimization problem, but that additional higher-order error terms arise. So long as the resulting modification to the first-order terms is not offset by these higher-order terms, the convergence rate will be improved. In particular, for linearly convergent fixed-point methods, an improved convergence rate from Anderson acceleration is expected; however, for methods converging quadratically, the convergence may be slowed. Additionally, the presented numerical results provide evidence for noncontractive fixed-point iterations that, while robustness of convergence with respect to choice of a uniform damping factor may be improved for the accelerated algorithm, robustness with respect to depth m as well as overall efficiency may be improved by using an adaptive damping factor based on explicit knowledge of the optimization gain θ_k, which can be easily computed at each iteration.

Acknowledgment. The authors would like to thank the anonymous referees for suggestions that improved the clarity of the results in this paper.

REFERENCES

[1] M. S. Alnæs, J. Blechta, J. Hake, A. Johansson, B. Kehlet, A. Logg, C. Richardson, J. Ring, M. E. Rognes, and G. N. Wells, *The FEniCS Project Version* 1.5, Archive of Numerical Software, 3 (2015), https://doi.org/10.11588/ans.2015.100.20553.

[2] H. An, X. Jia, and H. Walker, *Anderson acceleration and application to the three-temperature energy equations*, J. Comput. Phys., 347 (2017), pp. 1–19, https://doi.org/10.1016/j.jcp.2017.06.031.

[3] D. G. Anderson, *Iterative procedures for nonlinear integral equations*, J. Assoc. Comput. Mach., 12 (1965), pp. 547–560, https://doi.org/10.1145/321296.321305.

[4] F. Auteri, N. Parolini, and L. Quartapelle, *Numerical investigation on the stability of singular driven cavity flow*, J. Comput. Phys., 183 (2002), pp. 1–25, https://doi.org/10.1006/jcph.2002.7145.

[5] W. Bangerth, D. Davydov, T. Heister, L. Heltai, G. Kanschat, M. Kronbichler, M. Maier, B. Turcksin, and D. Wells, *The* `deal.ii` *library, version* 8.4, J. Numer. Math., 24 (2016), https://doi.org/10.1515/jnma-2016-1045.

[6] C. Brezinski, *Convergence acceleration during the* 20*th century*, J. Comput. Appl. Math, 122 (2000), pp. 1–21, https://doi.org/10.1016/S0377-0427(00)00360-5.

[7] P. R. Brune, M. G. Knepley, B. F. Smith, and X. Tu, *Composing scalable nonlinear algebraic solvers*, SIAM Rev., 57 (2015), pp. 535–565, https://doi.org/10.1137/130936725.

[8] H. Fang and Y. Saad, *Two classes of multisecant methods for nonlinear acceleration*, Numer. Linear Algebra Appl., 16 (2009), pp. 197–221, https://doi.org/10.1002/nla.617.

[9] M. Geist and B. Scherrer, *Anderson Acceleration for Reinforcement Learning*, EWRL 2018 – 4th European Workshop on Reinforcement Learning, October 2018, Lille, France.

[10] S. Hamilton, M. Berrill, K. Clarno, R. Pawlowski, A. Toth, C. T. Kelley, T. Evans, and B. Philip, *An assessment of coupling algorithms for nuclear reactor core physics simulations*, J. Comput. Phys., 311 (2016), pp. 241–257, https://doi.org/10.1016/j.jcp.2016.02.012.

[11] N. Higham and N. Strabic, *Anderson acceleration of the alternating projections method for computing the nearest correlation matrix*, Numer. Algorithms, 72 (2016), pp. 1021–1042, https://doi.org/10.1007/s11075-015-0078-3.

[12] C. Kelley, *Numerical methods for nonlinear equations*, Acta Numer., 27 (2018), pp. 207–287, https://doi.org/10.1017/S0962492917000113.

[13] W. Layton, *An Introduction to the Numerical Analysis of Viscous Incompressible Flows*, SIAM, Philadelphia, 2008, https://doi.org/10.1137/1.9780898718904.

[14] J. Loffeld and C. Woodward, *Considerations on the implementation and use of Anderson acceleration on distributed memory and GPU-based parallel computers*, in Advances in the Mathematical Sciences, Springer, Cham, 2016, pp. 417–436, https://doi.org/10.1007/978-3-319-34139-2_21.

[15] P. A. Lott, H. F. Walker, C. S. Woodward, and U. M. Yang, *An accelerated Picard method for nonlinear systems related to variably saturated flow*, Adv. Water Resour., 38 (2012), pp. 92–101, https://doi.org/10.1016/j.advwatres.2011.12.013.

[16] Y. Peng, B. Deng, J. Zhang, F. Geng, W. Qin, and L. Liu, *Anderson acceleration for geometry optimization and physics simulation*, ACM Trans. Graphics, 37 (2018), 42, https://doi.org/10.1145/3197517.3201290.

[17] S. Pollock, L. Rebholz, and M. Xiao, *Anderson-accelerated convergence of Picard iterations for incompressible Navier–Stokes equations*, SIAM J. Numer. Anal., 57 (2019), pp. 615–637, https://doi.org/10.1137/18M1206151.

[18] P. Stasiak and M. Matsen, *Efficiency of pseudo-spectral algorithms with Anderson mixing for the SCFT of periodic block-copolymer phases*, Eur. Phys. J. E, 34 (2011), 110, https://doi.org/10.1140/epje/i2011-11110-0.

[19] A. Toth, C. Kelley, S. Slattery, S. Hamilton, K. Clarno, and R. Pawlowski, *Analysis of Anderson acceleration on a simplified neutronics/thermal hydraulics system*, in Proceedings of the ANS MC2015 Joint International Conference on Mathematics and Computation (M&C), Supercomputing in Nuclear Applications (SNA) and the Monte Carlo (MC) Method, ANS MC2015 CD, 2015, pp. 1–12.

[20] A. Toth and C. T. Kelley, *Convergence analysis for Anderson acceleration*, SIAM J. Numer. Anal., 53 (2015), pp. 805–819, https://doi.org/10.1137/130919398.

[21] H. F. Walker and P. Ni, *Anderson acceleration for fixed-point iterations*, SIAM J. Numer. Anal., 49 (2011), pp. 1715–1735, https://doi.org/10.1137/10078356X.